FURTHER CHARACTERIZING THE EXTENT OF METAMORPHISM WITHIN THE DOMINION RANGE 08006 CO3 CHONDRITE T. J. Tenner[1], M. Kimura[2], and N.T. Kita[3], [1]Los Alamos National Laboratory, Los Alamos, NM 87545, USA. [2]National Institute of Polar Research, Tokyo, Japan, [3]WiscSIMS, Dept. of Geoscience, University of Wisconsin-Madison, Madison, WI 53706, USA (tenner@lanl.gov).

Introduction: Dominion Range (DOM) 08006 has been characterized as one of the least metamorphosed CO chondrites [1-4], with some features that are also similar to the ungrouped C3.00 chondrite Acfer 094 [5]. Specifically, DOM 08006 has a very high matrix-normalized abundance of presolar grains (240 ppm; [1]), high Cr_2O_3 and concentrations and low Cr_2O_3 standard deviations of its ferroan olivines [2], high C content (1.2 wt. %) and high H/C (0.465) [3], and a high abundance of matrix Fe-carbide and magnetite-bearing assemblages [4]. Collectively, these features are consistent with a meteorite that is less metamorphosed than Allan Hills (ALHA) 77307 (CO3.03), and more like Semarkona and Acfer 094, which have petrologic types of 3.01 and 3.00, respectively. Here, we provide additional characteristics of DOM 08006 that attest to its type 3.00-3.01 nature.

Sample and Methods: We investigated the DOM 08006,50 thin section loaned to us by NASA JSC. Backscattered electron (BSE) images were obtained using the JEOL JSM-7100F field emission scanning electron microscope at NIPR. Phase analyses were collected with the JEOL JXA8200 electron-probe microanalyzer at NIPR, with a focused beam (6 nA for silicates, 30 nA for opaques). Raman spectroscopy was also performed on feldspathic and silica-rich phases within 16 DOM 08006,50 chondrules, using a JASCO NRS 1000 at NIPR. A microscope focused the 532 nm excitation laser beam, and spectra were acquired from 200-1400 cm^{-1}.

Results and Discussion: *Degree of Secondary Alteration in chondrule, CAI, and AOA silicates:* Secondary anhydrous alteration of DOM 08006 chondrules can be compared those from CV chondrites; such alteration in CV chondrite chondrules includes secondary olivine zonation, replacement of plagioclase and/or glass by nepheline and/or sodalite, and replacement of enstatite by ferroan olivine [6,7]. Examination of DOM 08006,50 chondrules, as well as AOAs and CAIs, shows there is no evidence for any of these types of secondary alteration. There are no ferroan rims around olivine in AOAs, which suggests a 3.0 petrologic type (e.g. [8]). Additionally, while ALHA77307 chondrules abundantly contain phyllosilicates [9], DOM 08006,50 chondrules do not contain such phases.

Matrix grain size distribution: [10] note that when comparing matrix grain sizes, changes from fine-grained and non-porous textures, toward textures that are more porous and with coarser lath-like lithologies, are indicative of an increased degree of metamorphism. In this regard, DOM 08006,50 matrix is extremely fine-grained, with sub-micron features, and shows no porosity (Fig. 1). Among CO chondrites, DOM 08006 matrix appears most like that from Yamato (Y) 81020 (CO3.05) (e.g. Fig. 8a from [10]). According to the scheme put forth by [10], such a texture indicates the lowest extent of metamorphism.

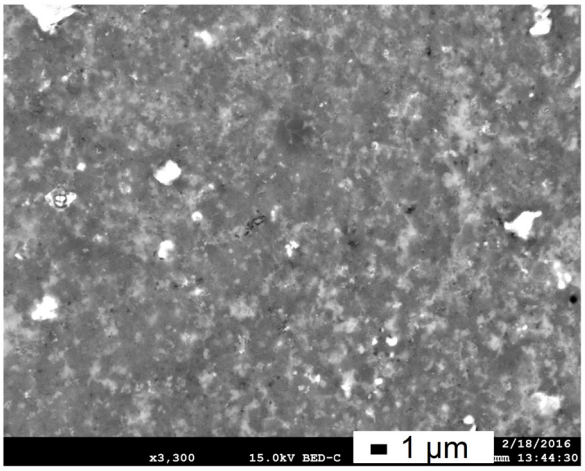

Fig. 1. BSE image of DOM 08006,50 matrix, revealing a fine-grained texture and low porosity.

Metal characteristics: Fe-Ni metal can be used to classify the extent of metamorphism in CO and ordinary chondrites [11]. Metals from 27 DOM 08006,50 chondrules were characterized, and are abundantly fine-grained and plessitic (having kamacite, tetrataenite, and Ni-rich regions). This texture is similar to metals in Semarkona chondrules (LL3.01). A plot of the average area of Ni-rich metal versus the number density of Ni-rich metal, shows that DOM 08006 is similar to that of Semarkona (Fig. 2a). Also, a plot of the number density of Ni-rich metal versus the Co of isolated Ni-rich metal/Co of chondrule kamacite shows that DOM 08006 is similar to Semarkona (Fig. 2b).

Raman spectroscopy: Raman spectroscopy of feldspathic phases in DOM 08006,50 chondrules reveals prominent peaks at 484 and 503 cm^{-1}, and in some scans, peaks at 281, 400, 427, 553, 681, and 974 cm^{-1}. All of these peaks are consistent with crystalline anorthite [12]; they are not consistent with anorthite polymorphs, nor secondary replacement phases like

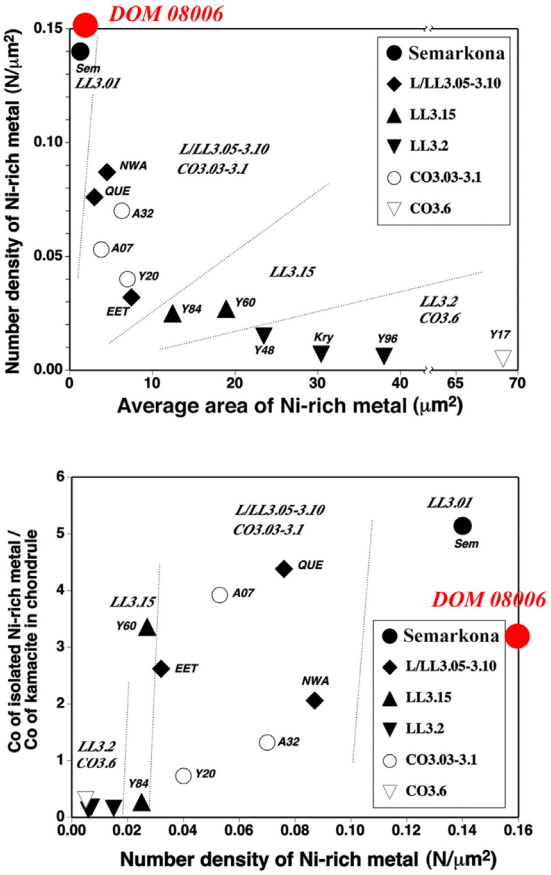

Fig. 2. Characteristics of Ni-rich metal, comparing those from DOM 08006 to other carbonaceous and ordinary chondrites. Plots follow Fig. 4. From [11].

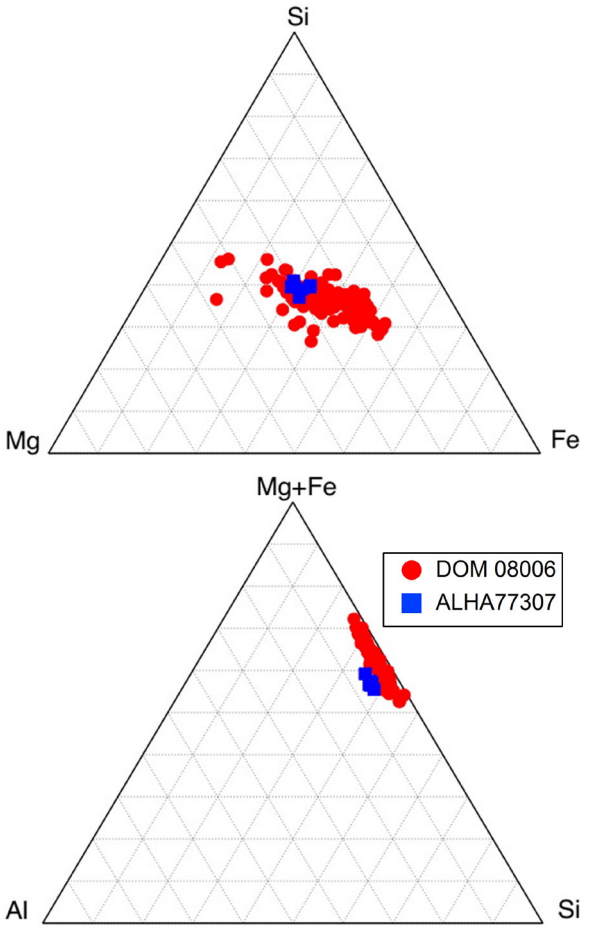

Fig. 3. Ternary plots of DOM 08006 and ALHA77307 matrix compositions. ALHA77307 data: [9].

nepheline and/or sodalite. Along with the presence of excess structural silica in DOM 08006 chondrule plagioclase [13], these features suggest the plagioclase avoided secondary metamorphism. Raman spectra of the silica-rich phase in DOM 08006,50 chondrules show prominent peaks at 230 and 416 cm^{-1}, consistent with α-cristobalite [14].

Matrix composition: Four different regions of matrix in DOM 08006,50 were analyzed by EPMA using a focused beam, and point analysis compositions are shown in Fig. 3. Generally the matrix of DOM 08006 is consistent with that from ALHA77307 [9]. However, DOM 08006 matrix is slightly depleted in Al. The reason for this is unclear, but we speculate it may be due to a relative deficit of matrix spinel.

Conclusions: Along with previous characterizations [e.g. 1-5], we find that DOM 08006 is the least metamorphosed CO3 chondrite, with a petrologic type below that of ALHA77307. At worst, we suggest that DOM 08006 is classified as a type 3.01 chondrite.

References: [1] Nittler L.R. et al. (2013) *LPS XLIV,* #2367 [2] Davidson J. (2014) *LPS XLV,* #1384. [3] Alexander C.M.O'D. (2018) *GCA*, *221*, 406-420. [4] Krot. A.N. et al. (2017) *LPS XLVIII*, #1084. [5] Simon S.B. and Grossman L. (2015) *MAPS*, *50*, 1032-1049. [6] Ikeda Y. and Kimura M. (1995) *Proc. NIPR Symp. Antarct. Meteorites*, *8*, 97-122. [7] Kimura M. and Ikeda Y. (1995) *Proc. NIPR Symp. Antarct. Meteorites*, *8*, 123-138. [8] Chizmadia L.J. (2002) *MAPS*, *37*, 1781-1796. [9] Ikeda Y. (1983) *Mem. Natl. Polar Res. Spec. Issue*, *30*, 93-108. [10] Komatsu M. et al. (2015) *MAPS*, *50*, 1271-1294. [11] Kimura M. et al. (2008) *MAPS*, *43*, 1161-1177. [12] Matson D.W. et al. (1986) *Am. Miner.*, *71*, 694-704. [13] Tenner T.J. (2017) *MAPS*, *52*, *S1*, A347. [14] Bates J.B. (1972) *J. Chem. Phys.*, *57*, 4042-4047.

This document is approved for unlimited release under LA-UR-18-20133.